Nonlinear Torque Observer for a Self-Energizing Clutch Actuator Using a Reaction Torque Estimation Approach

Jinsung Kim, *Member, IEEE*, and Seibum B. Choi, *Member, IEEE*

***Abstract*—Clutch torque estimation is an important problem in automotive transmission control. Particularly, a self-energizing clutch actuator system has a novel mechanism to amplify the clutch torque for reducing actuation energy. Instead of low energy consumption, the clutch torque is highly sensitive to the actuator stroke, which makes the torque detection difficult. The nonlinear disturbance observer is designed such that the clutch torque is estimated with guaranteeing asymptotic convergence by using the actuation motor position signal. This type of observer is based on the reaction torque estimation approach with respect to the actuator dynamics without considering vehicle driveline information. The experimental results show that the developed method is useful to identify the load characteristics of a self-energizing clutch actuator system.**

***Index Terms*—Automotive system, clutch actuator, drivetrain, nonlinear observer, torque estimation.**

I. Introduction

In automotive powertrain systems, actuator control performance is the main issue in automotive transmissions during gear-shifting and launch operation. Particularly in dry-clutch cases, this problem is closely related to how well a clutch torque control works [1], [2]. To obtain an effective solution of a clutch control, the clutch torque information during engagement should be needed for a feedback control design. However, direct clutch torque measurement is very difficult because torque transducers are quite expensive for practical automotive applications.

There are two approaches for clutch torque estimation in automotive systems. First, the driveline model-based approach is well known. The speed measurements at the engine, the shaft, and the wheel in the vehicle driveline are used to design an observer. Sliding mode observer is employed to identify the shaft torque [3]. Similarly, adaptive sliding observer estimates the turbine torque with torque converter parameters in automatic transmissions (AT) [4]. Neural network-based nonlinear observer is suggested incorporating extended Kalman filter as a training algorithm [5]. The shaft torque is estimated by using driveline dynamics dividing the engagement procedure into the stick–slip phase [6]. The major drawback of this approach is that the generated torque is detected only when both sides of the clutch disks remain slipping.

The second approach is to estimate a load torque in the actuator dynamics. In contrast with the driveline-based torque observer, the clutch torque during the engaged phase corresponds to the reaction torque to the actuator. Therefore, if the motor states and the load torque are known, the clutch torque could be identified by actuator information. It enables us to design the estimation system without considering vehicle driveline information. There are some researches in which electropneumatic and hydraulic actuators are used for this approach. For electropneumatic actuators, clutch load characteristics are investigated for preliminary study of a load estimation scheme [7]. Adaptive observers are designed for estimation of the clutch load, the friction coefficient, and the actuator velocity by a reduced order type [8], and full order type [9], respectively. Based upon estimated states from such observers, a dual-mode switched control is proposed [10], [11]. For electrohydraulic actuators, a clutch pressure observer is developed for ATs with clutch-to-clutch technology [12], [13]. The clutch pressure is estimated by the design of the clutch piston motion observer [14]. Regarding disturbances as unknown inputs, the observer is designed such that the resulting observer is input-to-state stable.

Compared with the results for clutch actuator systems equipped with electropneumatic or hydraulic actuators, relatively little attention has been paid for electromechanical clutch actuator systems due to the controllability problem and packaging issues. Until now, many automotive manufacturers seem to prefer hydraulic and electropneumatic actuators due to some practical advantages such as force multiplication, and lubrication. For these reasons, a clutch actuator system controlled by electromechanical actuators is at an early stage.

In this paper, some effort focuses on the systematic design of a load estimation of electromechanically controlled clutch actuator system particularly for the system that has a self-energizing mechanism [15]. Within an actuator control framework, the nonlinear observer for estimating the load torque of the actuator will be designed by using the motor position measurement only. Therefore, this paper belongs to the second approach for the clutch torque estimation.

Manuscript received March 26, 2014; revised November 8, 2014; accepted December 13, 2014. Date of publication August 24, 2015; date of current version October 21, 2015. Recommended by Technical Editor G. Liu. This research was supported by the Ministry of Science, ICT & Future Planning (MSIP), Korea, under the Convergence Information Technology Research Center (CITRC) support program (NIPA-2014-H0401-14-1001) supervised by the National IT Industry Promotion Agency (NIPA). This work was supported by the National Research Foundation of Korea (NRF) grant funded by the Korea Government (MSIP) (Grant 2010-0028680).

J. Kim is with Hyundai Motor Company, Hwasung 445-706, Korea (e-mail: jsk@kaist.ac.kr).

S. B. Choi is with the Department of Mechanical Engineering, Korea Advanced Institute of Science and Technology (KAIST), Daejeon 305-701, Korea (e-mail: sbchoi@kaist.ac.kr).

Color versions of one or more of the figures in this paper are available online at http://ieeexplore.ieee.org.

Digital Object Identifier 10.1109/TMECH.2014.2387070

The control-related issue of a self-energizing clutch actuator system (SECA) is the influence on the large reaction torque when the clutch is in contact. It implies that the torque phase is very short and the reaction torque exerted on the actuator has impact-like behavior. Thus, the force control design based only on the actuator position has limitations because of its engagement characteristic that is highly sensitive to the actuator position near the contact point. Thus, the development of the clutch torque observer will be useful for the purpose of the clutch engagement control design. Further, a SECA system has a self-energizing mechanism whose characteristic is nonlinear, and its instantaneous transition at the contact moment is problematic.

As the second approach, the linear disturbance observer (DOB) is one of popular methods for this approach [16]. In DOB formulation, external disturbances are lumped into additive disturbance. Then, the inverse of the transfer function of nominal plant and the input are filtered out by a low-pass filter to make a compensation signal inside the control loop. This filtered output can be considered as an estimated reaction force of the motor without force sensor [17]–[23].

However, DOB-based approach [16] has some limitation to overcome such problems because of noise sensitivity and limited bandwidth. Also, nonlinear DOB has been researched recently. Disturbances are identified based on the variable structure systems without the knowledge of its upper bound [24], where the class of applicable systems is limited. The DOB is simply designed with flexibility to be combined with a feedback controller [25]. However, it is required to assume that disturbances are linear exogenous system. A high-gain observer is incorporated with a sliding mode to estimate unknown inputs [26], which is sensitive to measurement noise.

The proposed nonlinear DOB has the robust integral of the sign of the error (RISE) structure that is a recently developed robust control method [27]. The RISE technique has been originally considered to guarantee continuous asymptotic tracking performance. It is highly robust against modeling uncertainties and has implicit learning characteristics [28], [29]. So, this method has been used to identify unknown parameters and detect a fault signal in dynamic systems as stated in literature [30] [31]. Inspired from a learning capability, a nonlinear DOB based on the RISE technique is designed to estimate the reaction torque of the clutch. Compared with other nonlinear approaches [24]–[26], the proposed method can be applied for unstructured disturbances with robustness to noise. First, we will design a nonlinear clutch torque observer based on the actuator velocity signal. Then, as the main purpose of this paper, a nonlinear clutch torque observer only using the position measurement will be designed as a mean of an observer-based clutch torque identification.

The outline of this paper is as follows. A brief overview and the experimental setup of a SECA system are given in Section II. For a comparison study and the illustration of the motivating example, a linear DOB-based approach for a clutch torque estimation will be discussed in Section III. In Section IV, a nonlinear DOB for a clutch torque estimation is developed with convergence analysis. The experimental results illustrate the clutch torque estimation by the proposed method. Finally, conclusions and future works are discussed in Section V.

TABLE I
DESCRIPTION OF CLUTCH ACTUATOR PARTS

No.	Name	No.	Name
A1	Friction disk	A11	Actuation neck
A2	Actuation plate (Rack1)	A12	Worm shaft
A3	Pinion gear	A13	Slot joint
A4	Pinion guide	A14	Thrust bearing
A5	Fixed plate (Rack2)	A15	Thruster
A6	Clutch cover	A16	Transmission Input shaft
A7	Damper Spring	A17	Lever
A8	Spline	A18	Ball screw
A9	Return spring	A19	Electric motor
A10	Bearing	A20	Encoder

II. PROBLEM FORMULATION

A. System Overview

A SECA system is recently developed as a new clutch mechanism for automated manual transmissions or dual clutch transmissions [15], [32], [33]. The schematic of a SECA system is shown in Fig. 1 with description of each part given in Table I. It can generate an additional force/torque to assist the engagement of a clutch disk. The amplification ability of the engagement torque depends on a self-energizing mechanism, which is configured by some wedge structure corresponding to the part of A2–A5 in Fig. 1(a) and (b). Such a mechanism can be implemented by a rack and pinion gear-set that enables a system to manipulate the clutch disk and gives a wedge structure at the same time. Because the resulting system can be operated effectively without having a diaphragm spring of conventional systems, some problems including the spring preload and nonlinearities are eliminated. Detailed descriptions of the operation principle of this mechanical system can be found on [15].

B. System Model

Since the actuation plate motion is very small in comparison with the motion of the motor rotor, it is assumed that the clutch disk built in the actuation plate is rigidly connected with the motor. Based upon this setting, the clutch actuator model can be derived with respect to the motor states. The following second-order model is utilized to describe the system dynamics based on the study [15]:

$$\bar{J}_m \dot{\omega}_m + q\omega_m + T_f(\omega_m) + T_l(\theta_m, \mu) = pu \tag{1}$$

where $\bar{J}_m$ is the equivalent moment of inertia, T_f is the motion friction, T_l is the load torque, and auxiliary variables p and q are defined as

$$\bar{J}_m \triangleq J_m + \frac{J_a}{N_g^2}, \qquad p \triangleq \frac{k_t}{R_m}, \qquad q \triangleq \frac{k_t k_m}{R_m}$$

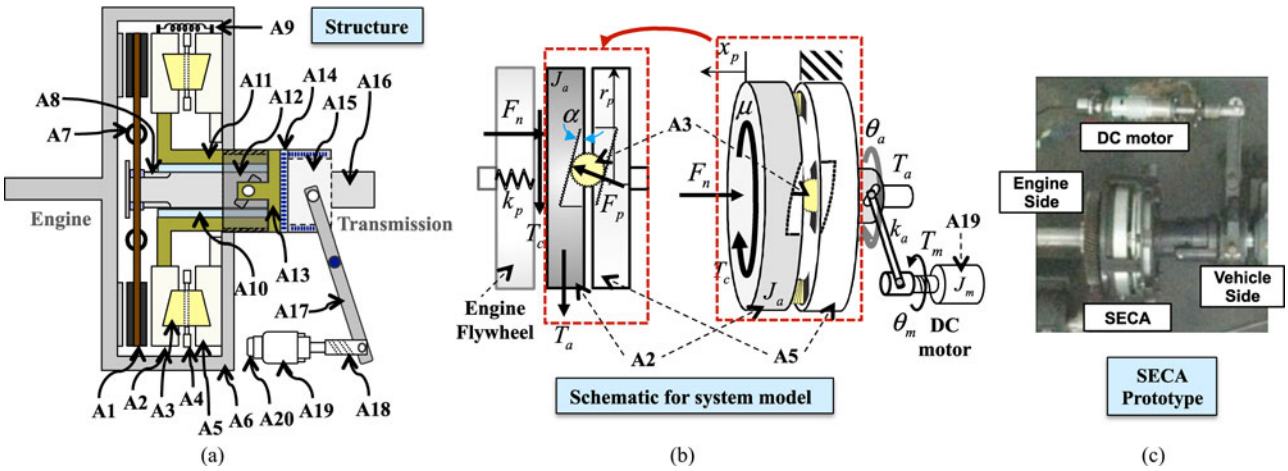

Fig. 1. SECA system: (a) Side view of the system structure. (b) Schematic of the system model. (c) Experimental prototype.

TABLE II
PARAMETERS AND VARIABLES FOR THE MODEL

Symbol	Name	Unit
J_m	Moment of inertia of the motor	kg·m^2
θ_m	Motor position	rad
ω_m	Motor velocity	rad/s
k_t	Motor torque constant	N·m/A
k_m	Back emf constant	V·s/rad
R_m	Motor resistance	Ω
N_g	Equivalent gear ratio	-
J_a	Moment of inertia of the actuation plate	kg·m^2
k_a	Stiffness of actuator mechanical part	N·m/rad
r_p	Pinion radius	m
α	Inclined surface angle (wedge angle)	deg
μ	Disk friction coefficient	$[0.27, 0.45]$
R_c	Clutch disk radius	m
F_n	Clutch normal force	N
T_c	Clutch torque	N·m

respectively. In (1), the motion friction model $T_f(\omega_m)$ depending only on the velocity is given by

$$T_f(\omega_m) = \sigma_1 \tanh(\sigma_2 \omega_m) + \sigma_3 \omega_m \tag{2}$$

where the Coulomb friction coefficient is given by σ_1 and σ_2, and σ_3 is the viscous friction parameter. The control input u in (1) is the applied voltage to track the desired actuator position trajectory. The controller used in this paper is the same as in [13] because we only study the observer design rather than the clutch controller. The other parameters and variables are given in Table II.

Let us briefly introduce the load torque model in (1). The load torque $T_l(\theta_m, \mu)$ in (1) is represented as

$$T_l(\theta_m, \mu) = r(\mu)\theta_m \tag{3}$$

where this actuator load can be parameterized by the equivalent stiffness $r(\mu)$ with respect to the motor position θ_m defined as

$$r(\mu) \triangleq \frac{k_a}{N_g^2}\left(\frac{k_b(\mu)}{k_b(\mu)+k_a}\right). \tag{4}$$

This is trivial that the clutch torque can be parameterized as the actuator stroke in order to find the clutch torque characteristic [10], [11], [34]

In (4), the auxiliary function $k_b(\mu)$ is defined for notational simplicity as

$$\xi(\mu) \triangleq 2r_p \tan\alpha - \mu R_c \tag{5a}$$

$$k_b(\mu) \triangleq \xi(\mu)(2r_p k_p \tan\alpha) \tag{5b}$$

where (5a) accounts for the clutch torque gain generated by a self-energizing mechanism, and (5b) implies the stiffness with respect to the rotational motion of the actuation plate. As shown in Fig. 1, the force balance in the steady state can be represented as

$$\begin{aligned} T_a &= 2r_p \tan\alpha F_n - \mu R_c F_n \\ &= \xi(\mu) F_n \end{aligned} \tag{6}$$

where T_a is the actuator driving torque so that the clutch normal force can be expressed as a function compliance between the motor and the mechanical subsystem

$$F_n = \frac{k_a}{\xi(\mu)}\left(\frac{\theta_m}{N_g} - \theta_a\right). \tag{7}$$

Considering a geometric relation, the actuator stroke x_p in Fig. 1 toward the engine flywheel can be defined as

$$x_p = 2r_p(\tan\alpha)\theta_a \tag{8}$$

and the clutch normal force is generated with actuator stiffness k_p as

$$F_n = k_p x_p. \tag{9}$$

Using (6)–(9), the relationship between the motor position θ_m and the actuation plate position θ_a is given by

$$\theta_a = \frac{k_a}{N_g(k_b(\mu)+k_a)}\theta_m \tag{10}$$

and the normal force is expressed as

$$F_n = \frac{k_a}{\xi(\mu)N_g}\left[\frac{k_b(\mu)}{(k_b(\mu)+k_a)}\right]\theta_m. \tag{11}$$

Since the load torque T_l is equivalent to $T_l = T_a/N_g$, combining (6) and (11) yields the compact form (3) and the relationship

$$T_l(\theta_m,\mu) = r(\mu)\theta_m = \frac{\xi(\mu)}{N_g}F_n = \frac{\xi(\mu)}{\mu R_c N_g}T_c \tag{12}$$

where (6) and $T_c = \mu R_c F_n$ are used. Note that if the clutch system does not have the self-energizing mechanism such that $\alpha = 0$, (12) simply becomes $T_l = -T_c/N_g$, which is the same as the case of traditional clutch system. For the detailed process, one can refer to the result [15], [33].

The state-space representation for the system (1) is given as follows:

$$\dot{x}_1 = x_2 \tag{13a}$$

$$\dot{x}_2 = \frac{1}{\bar{J}_m}\left[pu - qx_2 - T_f(x_2)\right] + d(t) \tag{13b}$$

where $x = [x_1, x_2]^T = [\theta_m, \omega_m]^T \in \mathbb{R}^2$, and $d(t)$ is the lumped unknown disturbance corresponding to the clutch torque load to the actuator, i.e.,

$$d(t) = -\frac{T_l(x_1,\mu)}{\bar{J}_m}. \tag{14}$$

Although the load torque can be parameterized as in (3), it is highly uncertain due to a clutch wear, temperature change, and material properties, which may lead to the actuator load torque variation. Thus, this reaction load of the actuator is taken into account as unknown time-varying disturbance $d(t)$ in (13b) and (14). Combining (12) and (14) yields the clutch torque that is the function of the actuator load

$$T_c = -\frac{\mu R_c N_g \bar{J}_m}{\xi(\mu)}d. \tag{15}$$

C. Experimental Setup

To validate a developed observer which will be introduced in the next section, a SECA system was set up in the driveline test bench as shown in Fig. 2. The driveline bench for verifications comprises a AC motor for automotive engine, a SECA system, a driveline shaft, and an equivalent vehicle inertia mass. In this test bench, the torque and speed sensors are used to measure the clutch torque and the shaft speed, respectively. It should be noted that since the direct measurement of the clutch torque is very difficult due to the physical limitation, the torque/speed sensors is installed at the shaft between the AC motor (engine) and the clutch. All data measurements from sensors in the experimental bench are acquired by using dSPACE MicroAutobox DS1401, where the sampling time is set to 1 ms.

For the clutch torque estimation, the proposed scheme will make use of the motor position measured from the incremental encoder having the resolution of 0.026º/revolution. The other measurements from sensors are used only for a validation purpose.

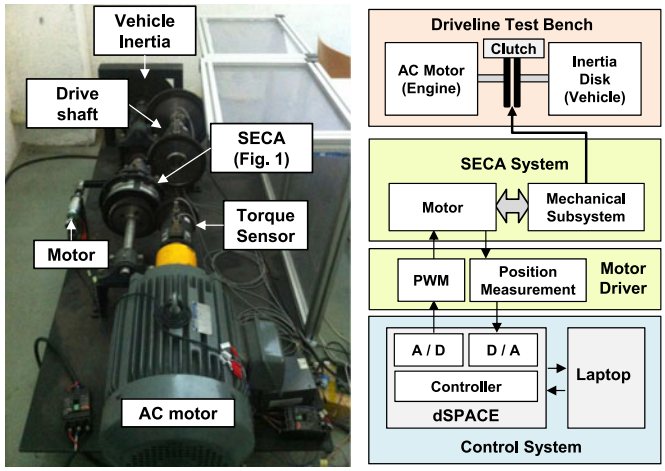

(a) (b)

Fig. 2. Driveline Test Bench with the SECA system: (a) Experimental setup. (b) Experimental system blocks diagram.

D. Objective

Since industrial manufacturers do not prefer the use of expensive torque sensors to transmission systems, a clutch torque observer should be required for control design and monitoring by utilizing the actuator dynamics.

The objective of this paper is to build a nonlinear observer for identifying the clutch torque of a SECA system, which corresponds to the reaction load of the actuator. The value of $T_l(\theta_m,\mu)$ of (1) implicitly includes the engagement torque and uncertain effect when the clutch comes into contact. Although the clutch torque is obtained by (11), it is difficult to find an accurate value because $k_b(\mu)$ is uncertain in real time. In a practical point of view, it seems intuitive that the value of $T_l(\theta_m,\mu)$ in (1) can be identified as a reaction load of the actuator. Thus, the proposed method requires that the actuator model is known, and the set of parameters should be identified accurately. The SECA system characteristics, modeling, and identification have been investigated in the preliminary study[15]. The available measurements are the motor voltage as an input, and the motor position as an output.

The main scope is the estimation methodology of a clutch torque. Thus, we assume that the position control in [15] is well adapted for the observer development in this paper. Rigorously, this assumption is acceptable because the semiglobal separation principle for nonlinear systems make it possible to deal with an observer problem without considering the plant stability [35], [36].

III. Clutch Torque Estimation Based on a Linear DOB

A. Linear DOB-Based Approach

In this section, a classical linear DOB is employed to design the reaction torque observer whose result corresponds to an equivalent clutch torque [17], [37]. The block diagram of this approach is shown in Fig. 3. From the result based on [17], [37],

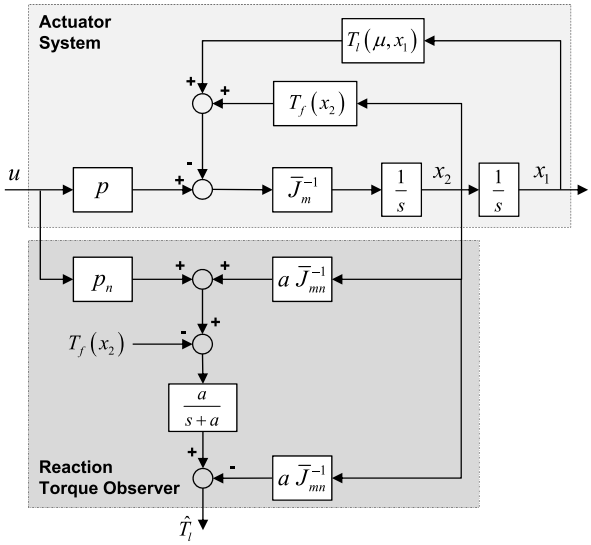

Fig. 3. Block diagram of the clutch torque observer based on the reaction torque observer.

the clutch load torque can be obtained as

$$\hat{T}_l = \frac{a}{s+a}\left(p_n u + a\bar{J}_{mn}x_2 - T_f(x_2)\right) - a\bar{J}_{mn} \qquad (16)$$

where a denotes the cutoff frequency of the reaction torque observer designed by the DOB, and $\bar{J}_{mn}$ and p_n are nominal values of actual variables of $\bar{J}_m$ and p, respectively. Note that the velocity x_2 is obtained from the numerical calculation of the position measurement x_1 in this approach.

B. Experimental Results

The clutch engagement test to validate of (16) is performed. Fig. 4(a) shows the speed synchronization between the engine (AC motor) and the vehicle (equivalent inertia) while the actuator position profile for a clutch contact in Fig. 4(b) is tracked by the SECA system. This engagement process in a launch case is divided into two stages: the torque phase when the clutch is contact but not slipping and the inertia phase when the clutch is slipping and the torque and kinetic energy are actually transferred to the shaft. The target actuator position corresponds to the torque value of 108 N·m.

The experimental result is shown in Fig. 4(c). The cutoff frequency a of the reaction torque observer is set to 60 rad/s. After 3.8 s, the steady-state value can be estimated successfully. However, the reaction behavior right after the clutch engagement cannot be captured effectively.

Remark 1: In a SECA system, the clutch torque is amplified by self-energizing effect from a wedge structure. This system can be interpreted as a high-stiffness mechanical system equivalently [15], where the contact motion from the free motion goes through hard environment. Therefore, the clutch torque during a contact transient period is highly sensitive to the actuator stroke. To estimate such a type of disturbance, an observer system should have the capability of transient performance recovery.

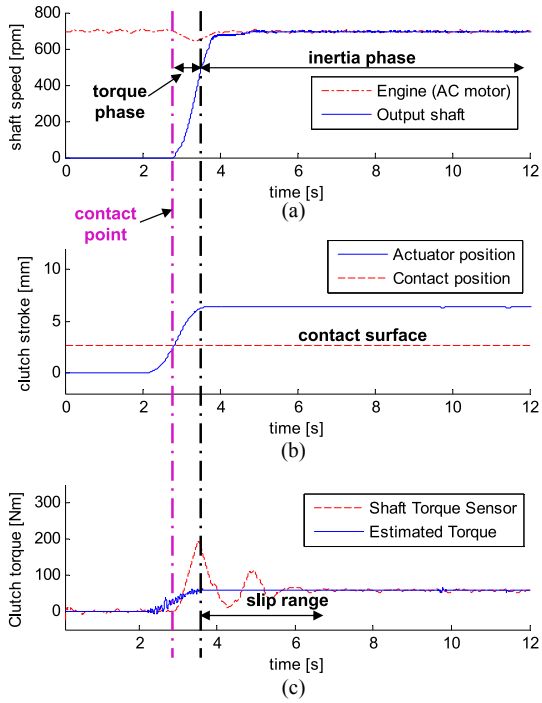

Fig. 4. Experimental results of clutch torque estimation by the reaction torque observer based on the DOB approach: (a) Driveline shaft speeds. (b) Position sequence of the clutch. (c) Clutch torque results.

In the LDOB approach, the major limitation is that transient performance of disturbance estimation is not recovered rather than the noise sensitivity [38]. Increasing the bandwidth of the LDOB regardless of measurement noise cannot solve this problem. As a result, estimation performance of a clutch torque during the engagement has been restricted. This motivates us to develop a nonlinear DOB that will be introduced in the subsequent section.

IV. Nonlinear Clutch Torque Observer

For a nonlinear torque observer design study, the velocity signal-based observer is first introduced under which both actuator position and velocity signals are available. Then, the position signal-based DOB will be proposed thereafter.

A. Velocity Signal-Based Nonlinear Torque Observer (VTOB)

The VTOB is designed with the velocity signal obtained from numerical differentiation of the position measurement. The following assumptions are made.

Assumption 1: There exist positive constants ρ_1 and ρ_2 such that given disturbances are twice continuously differentiable and have bounded derivatives with respect to time, i.e., $|\dot{d}(t)| < \rho_1, |\ddot{d}(t)| < \rho_2$.

Assumption 2: The control input is bounded, i.e., $u(t) \in \mathcal{U}$ for $t \geq 0$, where $\mathcal{U}$ is a compact set in $\mathbb{R}$.

Assumption 1 represents the condition for applying a nonlinear DOB that will be determined later. These parameters depend on the first and the second derivatives of a lumped disturbance. They correspond to the rate and the jerk limit of the clutch load

torque at the motor side. By using (14), the upper bounds ρ_1 and ρ_2 can be obtained as follows:

$$|\dot{d}(t)| = \frac{|\dot{T}_l|}{\bar{J}_m} < \rho_1, \qquad |\ddot{d}(t)| = \frac{|\ddot{T}_l|}{\bar{J}_m} < \rho_2 \tag{17}$$

where T_l is a function of the actuator position and the mechanical properties as defined in (3). Note that it can easily be verified experimentally in the clutch load torque measurement. Assumption 2 says that the control input is bounded for all nonnegative time within a compact set. Since the separation principle for observer design does not hold in nonlinear systems, such a setting guarantees the existence of the solution trajectory of the proposed observer with a plant dynamics. In addition, the nominal system dynamics with the initial condition $x(0)$ is known for observer design.

For the system (13), the velocity observer is given as

$$\dot{\hat{x}}_2 = \frac{1}{\bar{J}_m}\left[pu - qx_2 - T_f(x_2)\right] + \hat{d}(t) \tag{18}$$

where $\hat{d}(0) = -T_l(\theta_m, \mu)/\bar{J}_m = -r(\mu(0))\theta_m(0)/\bar{J}_m$. Although disturbance $d(t)$ depends on the actuator position, it is often inaccurate because the contact point of the clutch disk in uncertain. Hence, the reaction torque of the clutch is taken into account as a lumped disturbance d.

Let $e_2 \in \mathbb{R}$ be the velocity estimation error between (13) and (18), i.e.,

$$e_2 \triangleq x_2 - \hat{x}_2. \tag{19}$$

Using (13) and (18), the time derivative of the error can be written as

$$\dot{e}_2 = d - \hat{d} =: \tilde{d} \tag{20}$$

where $\tilde{d}$ is the disturbance error as defined earlier. It is clear that the error dynamics of the auxiliary velocity observer is equivalent to a nonlinear function of the disturbance estimation error under Assumptions 1 and 2 hold.

The nonlinear DOB $\hat{d} \in \mathbb{R}$ based on a RISE technique [27] is designed as

$$\begin{aligned}\hat{d}(t) = &\int_0^t (k_0+1)e_2(\tau)d\tau + \int_0^t k_1 \mathrm{sgn}(e_2(\tau))d\tau \\ &+ (k_0+1)e_2(t) - (k_0+1)e_2(0)\end{aligned} \tag{21}$$

where $\mathrm{sgn}(\cdot)$ is a standard signum function, and k_0 and k_1 are design parameters to be determined. Based on (12), (14), and (15), the clutch torque estimate can be obtained from

$$\hat{T}_c = -\frac{\mu R_c N_g \bar{J}_m}{\xi(\mu)}\hat{d}. \tag{22}$$

This implies that the clutch torque estimate in (22) including the self-energizing effect represented by $\xi(\mu)$, the lever effect, and parametric uncertainties is dynamically compensated from $\hat{d}$ calculated from (21). For the subsequent analysis, the filtered estimation error $r_1 \in \mathbb{R}$ is defined as

$$r_1 \triangleq \dot{e}_2 + e_2. \tag{23}$$

By taking the time derivative of (21), it can be shown that

$$\dot{\hat{d}} = (k_0+1)r_1 + k_1 \mathrm{sgn}(e_2(t)). \tag{24}$$

With (20), the time derivative of (23) is written as

$$\dot{r}_1 = \dot{d} - \dot{\hat{d}} + \dot{e}_2. \tag{25}$$

The estimation error system can be rewritten by substituting (24) into (25) as

$$\dot{r}_1 = \dot{d} - (k_0+1)r_1 - k_1 \mathrm{sgn}(e_2(t)) + \dot{e}_2. \tag{26}$$

Now, the following theorem states the convergence of the nonlinear DOB (21). This procedure is inspired from the RISE development [27].

Theorem 1: Under Assumptions 1 and 2, the estimated disturbance $\hat{d}$ in the auxiliary observer system (18) converges to the value d in the actual plant (13) in the sense that

$$\hat{d}(t) \to d(t) \quad \text{as} \quad t \to \infty \tag{27}$$

if the nonlinear observer gains in the VTOB (21) are chosen as

$$k_0 > 0, \quad k_1 > \rho_1 + \rho_2 \tag{28}$$

where ρ_1 and ρ_2 are given in Assumption 1.

Let $P_1(t) \in \mathbb{R}$ be a positive function defined as

$$P_1(t) := \zeta_{dv} - \int_0^t N_1(\tau)d\tau \tag{29}$$

where $\zeta_{dv} := k_1 e_2(0) - e_2(0)\dot{d}(0)$ and $N_1(\tau) \in \mathbb{R}$ is a function defined as

$$N_1(t) \triangleq r_1 \left[\dot{d} - k_1 \mathrm{sgn}(e_2(t))\right]. \tag{30}$$

In this step, we show that P_1 in (29) is positive with N_1 in (30) and the derivative of unknown disturbance d is canceled by the design parameter k_1. Together with definition (23), integration of (30) from 0 to t yields

$$\begin{aligned}\int_0^t N_1(\tau)d\tau = &\int_0^t \dot{e}_2(\tau)\dot{d}(\tau)d\tau - \int_0^t \dot{e}_2(\tau)k_1 \mathrm{sgn}(e_2(\tau))d\tau \\ &+ \int_0^t e_2(\tau)\left[\dot{d} - k_1 \mathrm{sgn}(e_2(\tau))\right]d\tau.\end{aligned} \tag{31}$$

The first term at the right-hand side in (31) can be integrated by parts. And, the second term is also integrated. Then, we have

$$\begin{aligned}\int_0^t N_1(\tau)d\tau = &\ e_2(t)\dot{d}(t) - e_2(0)\dot{d}(0) - k_1 e_2(t) + k_1 e_2(0) \\ &+ \int_0^t e_2(\tau)\left[\dot{d} - \ddot{d} - k_1 \mathrm{sgn}(e_2(\tau))\right]d\tau.\end{aligned} \tag{32}$$

Using the definition of ζ_{dv}, (32) is upper bounded by

$$\begin{aligned}\int_0^t N_1(\tau)d\tau \le &|e_2(t)|\left[\dot{d}(t) - k_1\right] + \zeta_{dv} \\ &+ \int_0^t |e_2(\tau)|\left[|\dot{d}| + |\ddot{d}| - k_1\right]d\tau.\end{aligned} \tag{33}$$

By applying the sufficient condition (28), the square bracket terms in (33) can be eliminated so that $N_1(t)$ satisfies the following inequality:

$$\int_0^t N_1(\tau)d\tau \le \zeta_{dv}. \tag{34}$$

This result clearly shows that there exists a positive function $P_1(t)$ in (29). Consider a positive definite Lyapunov function candidate $V_1(e_2, r_1, t) \in \mathbb{R}$

$$V_1(e_2, r_1, t) = \frac{1}{2}e_2^2 + \frac{1}{2}r_1^2 + P_1(t). \tag{35}$$

The time derivative of $\dot{V}_1$ is obtained as

$$\dot{V}_1(e_2, r_1, t) = e_2\dot{e}_2 + r_1\dot{r}_1 + \dot{P}_1(t). \tag{36}$$

Substituting (23) and (26) into (36) yields

$$\begin{aligned}\dot{V}_1(e_2, r_1, t) = \; & e_2(r_1 - e_2) + [\dot{e}_2 - (k_0+1)r_1]\, r_1 \\ & + \dot{P}_1(t) + r_1\left[\dot{d} - k_1\mathrm{sgn}(e_2(t))\right]. \end{aligned}\tag{37}$$

Using (23) and the fact that the time derivative of (29) is $\dot{P}_1(t) = -N_1(t)$, the expression (37) is rewritten as

$$\begin{aligned}\dot{V}_1(e_2, r_1, t) = \; & -e_2^2 - k_0 r_1^2 - N_1(t) \\ & + r_1\left[\dot{d} - k_1\mathrm{sgn}(e_2(t))\right]. \end{aligned}\tag{38}$$

By definition (30), the last two terms are canceled each other, and the expression (38) is reduced as

$$\dot{V}_1(e_2, r, t) = -e_2^2 - k_0 r_1^2 \le 0. \tag{39}$$

From (35) and (39), e_2 and $r_1 \in \mathcal{L}_\infty$. It is clear that $\dot{e}_2 \in \mathcal{L}_\infty$, and $e_2,\ r_1 \in \mathcal{L}_2$. Since the condition (28) is satisfied and Assumption 1 holds, it follows that $\dot{d} \in \mathcal{L}_\infty$. Therefore, the estimation-error dynamics (26) is bounded so that $\dot{r}_1 \in \mathcal{L}_\infty$. From this observation, $\dot{V}_1(e_2, r_1, t)$ is uniformly continuous. Barbalat's lemma can be used to show that $\dot{V}_1 \to 0$. It implies that $e_2 \to 0$ and $r_1 \to 0$ as $t \to \infty$. Based on the definition (20), it can be concluded that $\hat{d} \to d$.

Remark 2: The construction of the auxiliary velocity observer (18) aims at designing a disturbance estimator (21). The initial error $e_2(0)$ of the estimated velocity may cause a peaking signal of the disturbance estimate $\hat{d}$. Therefore, the initial value $\hat{x}_2(0)$ should be carefully chosen. Since the actuator system is initially at rest, $\hat{x}_2(0)$ can be easily selected as zero.

Remark 3: Theorem 1 gives the sufficient condition (28) for gains k_0 and k_1. Some knowledge of the actuator dynamics can be utilized as a known part of the observer. The gain k_1 is only considered for rejecting the disturbance estimation error. From Assumption 1, it is clear that the knowledge of ρ_1 and ρ_2 for determining k_1 can be obtained from the clutch torque rate and its derivative.

B. Position Signal-Based Nonlinear Torque Observer (PTOB)

A velocity measurement of mechanical systems is problematic due to the limitation of the production cost. Further, numerical differentiation requires higher resolution of the position encoder and may lead to the noise sensitivity issue. Therefore, the design of a clutch torque observer on the motor position measurement only is very important from the practical point of view. In the following, we propose a nonlinear PTOB as an extension to the VTOB. The PTOB has the following form:

$$\dot{\hat{x}}_1 = \hat{x}_2 + \gamma(t) \tag{40a}$$

$$\dot{\hat{x}}_2 = \frac{1}{\bar{J}_m}\left[pu - q\hat{x}_2 - T_f(\hat{x}_2)\right] + L\gamma(t) + \hat{d}(t) \tag{40b}$$

$$\begin{aligned}\hat{d} = & \int_0^t (k_0+2)e_2^*(\tau)d\tau + \int_0^t k_1\mathrm{sgn}(e_2^*(\tau))d\tau \\ & +\ (k_0+2)e_2^*(\tau) - (k_0+2)e_2^*(0)\end{aligned}\tag{40c}$$

where L is a positive constant, k_0 and k_1 are design parameters for disturbance estimation, respectively. Note that $\gamma(t)$ is the state observer injection to be designed later. As in the VTOB case, the estimated clutch torque $\hat{T}_c$ is calculated from (40c) with the relationship (22). Let the estimation error be $e := x - \hat{x} \in \mathbb{R}^2$. From (13) and (40), the observer error dynamics is expressed as

$$\dot{e}_1 = e_2 - \gamma(t) \tag{41a}$$

$$\dot{e}_2 = \; -\bar{q}e_2 - \tilde{T}_f(x_2, \hat{x}_2) - L\gamma(t) + \tilde{d}(t) \tag{41b}$$

where $\bar{q} = q/\bar{J}_m, \tilde{T}_f(x_2, \hat{x}_2) = [T_f(x_2) - T_f(\hat{x}_2)]/\bar{J}_m, \tilde{d} = d - \hat{d}$, and e_2^* is defined as $\{e_2^* \in \mathbb{R} | (e_1, e_2) = (0, e_2)\}$. The injection γ for the state observer part is first designed such that the output estimation error e_1 becomes zero. Then, the error system is evolved on the set $\mathcal{A} = \{e \in \mathbb{R}^2 | (e_1, e_2) = (0, e_2)\}$. The gain L in (41b) plays a role of stabilization of e_2 dynamics when the error system (41) belongs to $\mathcal{A}$. Notice that the design of L depends on the other parameters that will be introduced later.

The disturbance is identified from the signal e_2^*. Here, the question is how to obtain the signal $e_2^* \in \mathcal{A}$. In this case, e_2^* is not available directly while the position is measurable only. The idea to solve this problem comes from an equivalent control method in sliding control theory [39], [40]. It is a technique for obtaining the solution of differential equations of slow motion that is obtained by a large feedback gain that is injected into fast motion system [39]. In this case, the output error dynamics (41a) is taken into account as fast dynamics while (41b) describe slow motion relatively. When applying a high-gain feedback γ to the dynamic error system (41), the trajectory of the error dynamics reaches the set $\mathcal{A}$. Since the motion of the solution is relatively slow in $\mathcal{A}$, it can be taken by solving a low-pass filter [40] so that e_2^* is obtained from

$$\epsilon\dot{e}_2^* = \; -e_2^* + L\gamma(t) \tag{42}$$

where ϵ is a design parameter for determining the bandwidth of the filter.

To analyze the error convergence, we introduce a nonsingular coordinate transformation $\xi \triangleq Te$ with

$$T \triangleq \begin{bmatrix} 1 & 0 \\ -L & 1 \end{bmatrix} \tag{43}$$

defined as

$$\xi_1 = e_1 \tag{44a}$$

$$\xi_2 = e_2 - Le_1 \tag{44b}$$

where $\xi = [\xi_1 \xi_2]^T$ with $\xi_1 \in \mathbb{R}$ and $\xi_2 \in \mathbb{R}$. In the transformed coordinate, the observer error dynamics (41) is described by

$$\dot{\xi}_1 = \xi_2 + L\xi_1 - \gamma(t) \tag{45a}$$

$$\dot{\xi}_2 = -(\bar{q} + L)L\xi_1 - (\bar{q} + L)\xi_2 - \tilde{T}_f + \tilde{d} \tag{45b}$$

where the state observer injection $\gamma(t)$ is designed as

$$\gamma(t) = \phi_1 e_1(t) \tag{46}$$

with a positive constant ϕ_1 for state estimation injection gain, and $\tilde{d} \triangleq d - \hat{d}$ is the disturbance estimation error. Let $r_2 \in \mathbb{R}$ be the filtered estimation error defined as

$$r_2(t) \triangleq \dot{\xi}_2 + \xi_2 \tag{47}$$

and $r_2^* \in \mathbb{R}$ is similarly defined as

$$r_2^*(t) \triangleq \dot{\xi}_2^* + \xi_2^* \tag{48}$$

on a set $\mathcal{A}$. After utilizing (48) based on (40c), the time derivative of $\hat{d}$ is

$$\dot{\hat{d}}(t) = (k_0 + 2)r_2^*(t) + k_1 \text{sgn}(\xi_2^*(t)). \tag{49}$$

The time derivative of (47) is given as

$$\dot{r}_2(t) = \dot{F}_2(\xi, \dot{\xi}, x, \dot{x}) + \dot{\xi}_2 + \dot{d} - \dot{\hat{d}} \tag{50}$$

where $\dot{F}_2(\xi, \dot{\xi}, x, \dot{x}) = -(\bar{q} + L)L\dot{\xi}_1 - (\bar{q} + L)\dot{\xi}_2 - \dot{\tilde{T}}_f$. Substituting (49) into (50) yields

$$\begin{aligned}\dot{r}_2(t) = \; & \dot{F}_2(\xi, \dot{\xi}, x, \dot{x}) + \dot{\xi}_2 + \dot{d} \\ & - (k_0 + 2)r_2^* - k_1 \text{sgn}(\xi_2^*).\end{aligned} \tag{51}$$

For the subsequent convergence analysis, an auxiliary function $P_2(t) \in \mathbb{R}$ is defined as

$$P_2(t) := \zeta_d - \int_0^t N_2(\tau)d\tau \tag{52}$$

where $N_2(\tau) \in \mathbb{R}$ and ζ_d are defined as

$$N_2(\tau) \triangleq r_2 \left(\dot{d}(\tau) - k_1 \text{sgn}(\xi_2^*(\tau)) \right) \tag{53}$$

$$\zeta_d \triangleq k_1 e_2^*(0) - Lk_1 e_1(0) - e_2(0)\dot{d}_2(0). \tag{54}$$

The augmented vector $z \in \mathbb{R}^3$ is defined as

$$z \triangleq [\xi_1 \xi_2 r_2]^T. \tag{55}$$

And, some parameters are defined such that

$$\varphi_1 > (\bar{q} + L)L + L \tag{56}$$

$$\varphi_2 \triangleq \frac{(2 + k_0)^2}{2}\varphi_1^2 \tag{57}$$

$$\phi_1 \geq \frac{1}{2} + L + \varphi_2^2 + \beta_1 \tag{58}$$

where β_1 is a certain positive constant. The following theorem states the convergence of overall estimation error dynamics of the PTOB.

Theorem 2: Under Assumptions 1 and 2, the position-based observer presented in (40) ensures that the state estimation error $\tilde{x}$ and $\tilde{d}$ converge to zero in the sense that

$$\xi_1, \xi_2, r_2, \text{and } \tilde{d} \to 0 \quad \forall v(0) \in \mathcal{D}$$

where the domain of the compact set $\mathcal{D}$ can be made large arbitrarily by k_0 for the initial condition and the trajectory of the plant dynamics if the gain k_1 satisfies

$$k_1 > \rho_1 + \rho_2 \tag{59}$$

and k_0 and ϕ_1 satisfy the relationship (56) and (58).

Lemma 1: If the condition (59) holds for k_1 with sufficiently small ϵ in (42), then the following inequality for the integral of N_2 defined in (53) can be satisfied:

$$\int_0^t N_2(\tau)d\tau \leq \zeta_d \tag{60}$$

where ζ_d is defined in (54). The proof of the Lemma 1 is given in Appendix. The following proof is for Theorem 2.

Proof: Consider the composite vector $v \in \mathbb{R}^4$ defined as

$$v \triangleq [z^T \sqrt{P}]^T \tag{61}$$

where $z \in \mathbb{R}^3$ is defined in (55). Let $V_2(v, t) \in \mathbb{R}$ be a positive definite Lyapunov function candidate

$$V_2(v, t) = \frac{1}{2}\xi_1^2 + \frac{1}{2}\xi_2^2 + \frac{1}{2}r_2^2 + P_2(t) \tag{62}$$

which satisfies the inequalities

$$U_1(v) \leq V_2(v, t) \leq U_2(v) \tag{63}$$

where $U_1(v) \triangleq 0.5\|v\|^2$ and $U_2(v) \triangleq \|v\|^2$ are continuous positive definite functions. Taking the time derivative of (62) is

$$\dot{V}_2(v, t) = \xi_1\dot{\xi}_1 + \xi_2\dot{\xi}_2 + r_2\dot{r}_2 + \dot{P}_2. \tag{64}$$

Along with the trajectory of (45) with (47), (51) and (52), the expression (64) is rewritten as

$$\begin{aligned}\dot{V}_2(v, t) = \; & \xi_1(\xi_2 + L\xi_1 - \gamma) - \xi_2^2 + r_2^2 + r_2\dot{F}_2(\xi, \dot{\xi}, x, \dot{x}) \\ & - N_2 - (k_0 + 2)r_2 r_2^* + \left[\dot{d}_2(\tau) - k_1 \text{sgn}(e_2^*(\tau)) \right]\end{aligned} \tag{65}$$

where the last terms in the bracket and the term N_2 are canceled each other based on (52) and (53). Adding and subtracting $(k_0 + 2)r_2^2$ to (65) yields

$$\begin{aligned}\dot{V}_2(v, t) = \; & \xi_1\xi_2 + \xi_1(L\xi_1 - \gamma) - \xi_2^2 + r_2\dot{F}_2(\xi, \dot{\xi}, x, \dot{x}) \\ & + (k_0 + 2)r_2(r_2 - r_2^*) - k_0 r_2^2 - r_2^2.\end{aligned} \tag{66}$$

From the definitions (47) and (48), it follows that

$$r_2 - r_2^* = \dot{\xi}_2 - \dot{\xi}_2^* + \xi_2 - \xi_2^*. \tag{67}$$

From (44b) and (45b) with the definition $\{\xi_2^* \in \mathbb{R} | (\xi_1, \xi_2) = (0, \xi_2)\}$, (67) is divided into

$$\dot{\xi}_2 - \dot{\xi}_2^* = -(\bar{q} + L)L\xi_1 \tag{68}$$

$$\xi_2 - \xi_2^* = -L\xi_1 \tag{69}$$

where $\dot{\xi}_2^*$ and ξ_2^* can be obtained from (45b) and (44b) with $\xi_1 = 0$, respectively, (67) can be rewritten as $r_2 - r_2^* = -[(\bar{q} + L)L + L]\xi_1$. Therefore, the following inequality can be developed:

$$|r_2 - r_2^*| \leq -\varphi_1 |\xi_1| \tag{70}$$

where φ_1 is selected to satisfy (56). Since $\dot{F}_2(\xi, \dot{\xi}, x, \dot{x})$ is continuously differentiable, there exists a positive, globally invertible, nondecreasing function $\rho(\cdot) \in \mathbb{R}$ such that

$$\dot{F}_2(\xi, \dot{\xi}, x, \dot{x}) \leq \rho(\|z\|)\|z\|. \tag{71}$$

Using (70), (71), and the fact that $\xi_1\xi_2 \leq (1/2)\xi_1^2 + (1/2)\xi_2^2$

$$\begin{aligned}\dot{V}_2(v,t) \leq -\gamma\xi_1 + \left(\frac{1}{2} + L\right)\xi_1^2 - \frac{1}{2}\xi_2^2 + r_2\rho(\|z\|)\|z\| \\ + \varphi_1(k_0 + 2)|r_2||\xi_1| - k_0 r_2^2 - r_2^2.\end{aligned} \tag{72}$$

Using the following upper bound:

$$\varphi_1(k_0 + 2)|r_2||\xi_1| \leq \varphi_2^2\xi_1^2 + \frac{1}{2}r^2 \tag{73}$$

where φ_2 is defined in (57), and the applying γ as in (46), the expression (72) is upper bounded as follows:

$$\begin{aligned}\dot{V}_2(v,t) \leq \; & -\left(\phi_1 - \frac{1}{2} - L - \varphi_2^2\right)\xi_1^2 - \frac{1}{2}\xi_2^2 - \frac{1}{2}r^2 \\ & + \left[r_2\rho(\|z\|)\|z\| - k_0 r_2^2\right].\end{aligned} \tag{74}$$

The state observer gain ϕ_1 can be selected to satisfy the inequality (58). Completing the square for the last bracket term in (74) and the gain selection in (58) yield

$$\dot{V}_2(v,t) \leq \; -\beta_z\|z\| + \frac{1}{4k_0}\rho^2(\|z\|)\|z\|^2 \tag{75}$$

where $\beta_z = \min\{\beta_1, 1/2\}$. Let $U(v)$ be a positive semi-definite function, and $\mathcal{D} \subset \mathbb{R}^4$ a domain containing $v(t) = 0$ defined as

$$\mathcal{D} := \left\{v(t) \in \mathbb{R}^4 \mid \|v\| \leq \rho^{-1}\left(\sqrt{2k_0\beta_z}\right)\right\}. \tag{76}$$

It follows from (75) that $\dot{V}_2(v,t) \leq -U(v)$ for $v \in \mathcal{D}$ defined in (76). Based on (62) and (75), it can be shown that $\xi_1(t)$, $\xi_2(t)$, and $r_2(t) \in \mathcal{L}_\infty$ in $\mathcal{D}$. From (45), (49), and Assumption 1, $\dot{\xi}_1(t)$, $\dot{\xi}_2(t) \in \mathcal{L}_\infty$ in $\mathcal{D}$. From (47), (49), and (50), it can also be shown that $\dot{r}_2 \in \mathcal{L}_\infty$ in $\mathcal{D}$. Since $\dot{\xi}_1(t)$, $\dot{\xi}_2(t)$, and $\dot{r}_2 \in \mathcal{L}_\infty$ in $\mathcal{D}$, $U(v)$ is uniformly continuous in $\mathcal{D}$.

Let $\mathcal{S} \subset \mathcal{D}$ be a compact subset defined as

$$\mathcal{S} := \left\{v(t) \in \mathcal{D} \mid U_2(v) < \Psi_1\left(\rho^{-1}\left(\sqrt{2k_0\beta_z}\right)\right)^2\right\} \tag{77}$$

where the size of this domain depends on any initial conditions and the DOB gain k_0. Theorem 8.4 in [41] can be used to show the semiglobal error convergence in the sense that

$$c\|z\|^2 \to 0 \qquad t \to \infty \quad \forall v(0) \in \mathcal{S}. \tag{78}$$

Based on (55), the statement (78) implies that

$$\xi_1, \xi_2, \text{and } r_2 \to 0 \qquad t \to \infty \quad \forall v(0) \in \mathcal{S}. \tag{79}$$

From the definition of (47) and (50), the following conclusion is the immediate consequence of (79):

$$\tilde{d} \to 0 \qquad t \to \infty \quad \forall v(0) \in \mathcal{S}. \tag{80}$$

■

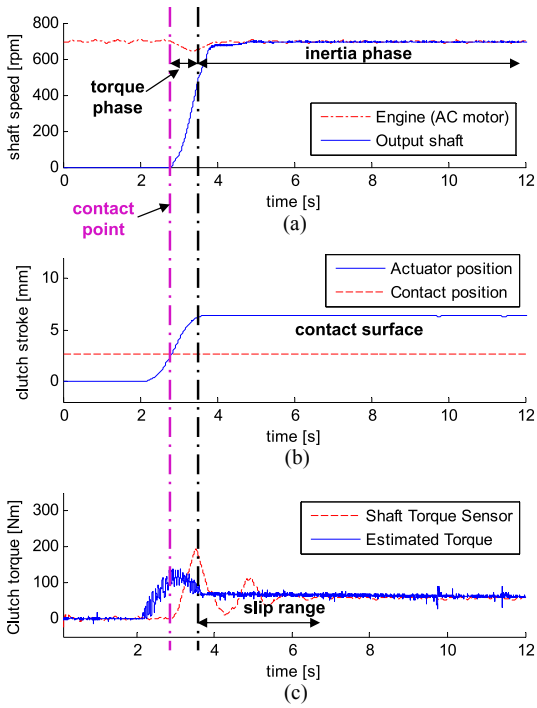

Fig. 5. Experimental results of clutch torque estimation by velocity signal-based observer.

C. Experimental Results

As mentioned before, the controller used for observer validation in this paper is the same in [13] for tracking the desired actuator position trajectory.

1) VTOB: To verify the proposed estimation methods, clutch engagement experiments are performed. The same actuator profile and the driveline data set in Section III-B are used to compare the result with the linear DOB case. Fig. 5 shows the torque estimation result by VTOB with the tuning parameters given in Table III. Based on (14), the estimated value obtained is scaled by the equivalent moment of inertia of the motor. Even though the estimated torque value corresponds to the actual one qualitatively, the resulting signal has too much noise and some spikes on the signal are observed. This is mainly due to the fact that the velocity signal is obtained from the numerical differentiation of the position measurement. It is undesirable because the estimated torque is contaminated by noise. As a result, it can be shown that the VTOB is effective when the velocity measurement is very accurate.

TABLE III
OBSERVER DESIGN PARAMETERS

Parameter	VTOB	PTOB
L	–	1.2
ϕ_1	–	4.2
k_0	0.69	1.8
k_1	10^{-3}	0.02
ϵ	–	0.016

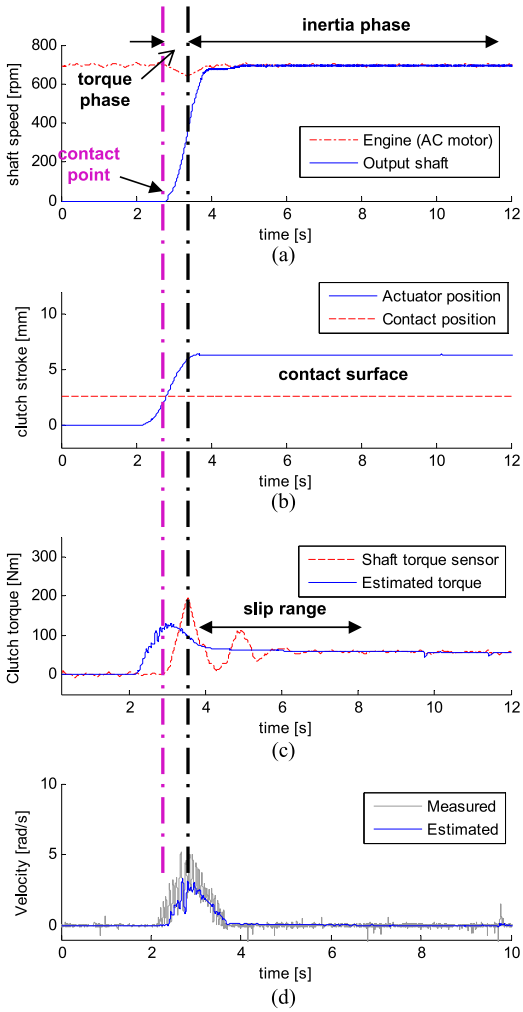

Fig. 6. Experimental results of clutch torque estimation by position signal-based observer: (a) Driveline shaft speeds. (b) Position sequence of the clutch. (c) Clutch torque estimation. (d) Velocity estimation.

2) PTOB: The results of the PTOB is shown in Fig. 6. In Assumption 1, The upper bounds ρ_1 and ρ_2 depend on the clutch torque rate and its derivative which are selected by the specified control input such that $|\dot{T}_l| = 0.14$ N·m/ms and $|\ddot{T}_l| = 0.001$ N·m/ms^2. With this and (12), it can be determined that $\rho_1 = 0.44$ and $\rho_2 = 3.13$e-4 under which the control implementation were performed at the sampling time of 1ms.

Based on this setting, the gain tuning process can be summarized as follows. Initially, L and φ_1 are chosen based on given system parameters, (56), and (57). Then, ϕ_1 can be computed from (58). However, a conservative Lyapunov-based analysis leads to the high gains of ϕ_1 and k_1. If the estimated value exhibited overshoot at the initial period, the smaller ϕ_1 and k_1 were selected iteratively. As a result, some gains do not satisfy the *sufficient* conditions provided in Theorem 2. Table III shows the selected design parameters.

TABLE IV
MAXIMUM AND AVERAGE ERRORS FOR THE CLUTCH TORQUE OBSERVERS IN THE ENGAGED PHASE ($3.52 \leq t \leq 12$)

Estimation error	DOB	VTOB	PTOB
Average error [N·m]	22.13	21.50	18.88
Maximum error [N·m]	140.87	129.62	96.95

Compared with the VTOB, the velocity estimation can be obtained additionally as shown in Fig. 6(d). Also, the PTOB achieves superior torque estimation performance than the VTOB case. In Fig. 6(c) for Theorem 2, the engagement torque can be identified without noise problems. As shown in Fig. 6(c), measuring the shaft torque to indirectly obtain the clutch torque may yield the delayed response whose extent depends on the torque sensor quality. The use of the proposed observer can also solve this problem without any extra cost.

3) Comparative Study: The maximum and average estimation errors are investigated in Table IV for a comparison study. The validity domain for observer verifications is considered in the time duration of $3.52 \leq t \leq 12$, where the clutch is engaged and the kinetic energy of the engine (AC motor in this setup) is transferred to the vehicle inertia. The experimental data in Table IV shows that the PTOB results in the reduced estimation error compared with other methods.

In the VTOB, the velocity signal of the actuator is utilized as a correction term. As shown in Theorem 1, the VTOB has global convergence of the estimation error dynamics under Assumptions 1 and 2 hold. It implies that the VTOB in (18) and (21) can identifies unknown disturbance as a clutch torque when the velocity signal is available.

On the other hand, the PTOB additionally requires the velocity estimation because a given system does not allow full state measurement in practice. In other words, the PTOB enables the velocity signal to be reconstructed as well as the clutch torque as an unstructured disturbance is estimated.

This additional estimation of the actuator velocity results in reducing the noise sensitivity. The VTOB (21) utilizes the feedthrough term $e_2(t)$ including the velocity measurement $x_2(t)$ so that the disturbance estimate $\hat{d}$ is corrupted by noise. The PTOB (40c) uses $e_2^*(t)$ that is obtained from a low-pass filter (42) based on the equivalent control-like method. Thus, the noise filtering capability of the PTOB can be adjusted from the design parameter ϵ in (42). The torque estimation result shown in Fig. 6(c) shows that the noise is well suppressed.

However, such a setting makes the PTOB system even more complex compared with the VTOB. Theorem 2 shows that the PTOB guarantee the semiglobal convergence. The region of attraction can be defined as $\mathcal{S}$ in (77), which is a compact subset of $\mathcal{D}$ ensuring the error convergence of the PTOB. The gain k_0 turns out to be the design parameter to adjust the size of

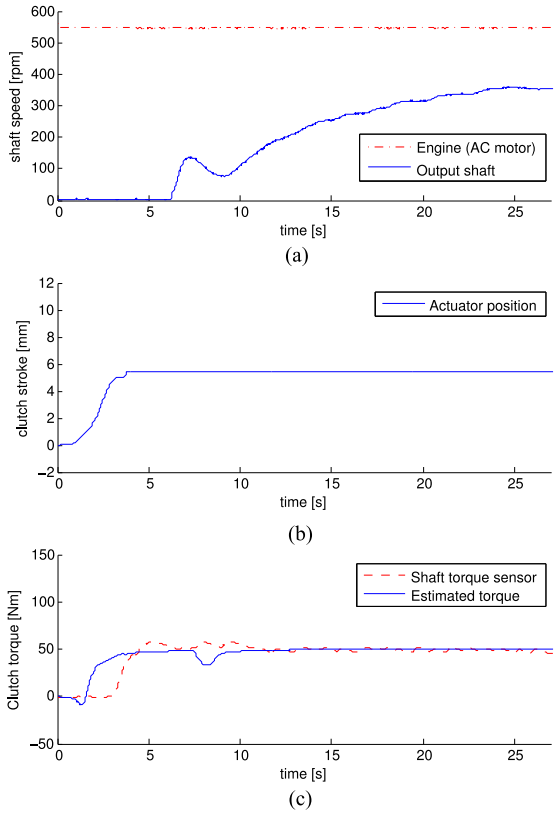

Fig. 7. Experimental results of clutch torque estimation by position signal-based observer when the ac motor is rotating in reverse for the case of the *self-de-energizing* effect: (a) Driveline shaft speeds. (b) Position sequence of the clutch. (c) Clutch torque estimation.

domain of the error convergence verified in (76) and (77). The larger size of domain can be obtained arbitrary by increasing k_0. However, k_0 should be carefully chosen with considering relationship (56)–(58).

It is also interesting to see the engine brake situation, where the torque direction is reversed. Particularly for the SECA system, the ac motor rotating in reverse can describe the engine brake situation indirectly. Also, this is equivalent to the self-de-energizing case in the SECA system. The clutch torque by reverse torque transmission is also identified by the reaction torque estimation of the actuator.

In this case, the clutch slip is excessive because certain amount of the applied torque is reduced by the self-de-energizing effect. Thus, the estimated torque in this case is less than the self-energizing case. Fig. 7 shows that the clutch slip occurs because the applied torque is reduced by the self-reenergizing effect. The measured and the estimated torque are small in order to achieve the clutch speed synchronization. The torque is estimated well because the proposed observer is just based on the actuator reaction torque.

4) Parametric Study: To discuss the robustness with respect to parametric uncertainties in the nominal model, the estimation performance is investigated with parameter variations of the motion friction function $T_f(\omega_m)$ in (1). When the nominal values of σ_2 and σ_3 in (2) are increased up to 20%, these variations do not affect the estimation performance as shown in Figs. 8(b) and 9(b). There are only slight variations that are not significant.

Fig. 8(a) and 9(a) show the effect of σ_1 variation increasing up to 20% from the nominal value. The VTOB in Fig. 8(a) shows that the result is robust against the modeling uncertainties. However, it is still highly sensitive to noise.

The PTOB with uncertain model yields the torque estimation error of 20% as shown in Fig. 9(a). Since the velocity estimate is obtained from the part of the state observer, the modeling uncertainty gives rise to erroneous state estimations. As a result, the disturbance, which is identified based on the velocity estimate, becomes erroneous as well. Therefore, the system model should be accurate for utilizing the PTOB.

Remark 4: In our experimental setup, there is a short time delay between the estimated torque and the actual value. It is caused by indirect measurement of the clutch torque, which is calculated from the shaft torque while the clutch is slipping. This is originated from the fact that the small amount of shaft torsion in the initial period of a clutch slip is not detectable because its quantity depends on the specified sensor resolution.

However, it is sufficient to verify the clutch torque from this configuration for the validation purpose. In automotive manufacturers, the clutch torque of a dry-friction disk is also indirectly validated by the drive shaft torque measurement due to the cost and physical limitation of sensor installation. In Figs. 5–9, it has been shown that the estimated torque converged to the measured shaft torque after the clutch makes contact with. Generally, it is important that the clutch torque is physically meaningful after the dry-frictional disk slip occurs.

Remark 5: The clutch torque characteristics can be interpreted with respect to the actuator stroke. Therefore, the resulting estimate of the clutch torque can be obtained without the effect of the driveshaft compliance. It is extremely useful as real-time torque information for the torque characteristic curve update. Because such torque characteristics are defined in the actuator layer, the torsional mode at the driveshaft is not necessary [34].

To estimate the effect of the driveshaft torsional stiffness and damping, it is better to consider the driveline model-based approach, where the transmitted torque in clutch can be identified based on the engine torque. A more detailed description can be found on our recent study [42].

V. Conclusion

A nonlinear DOB is designed to estimate the clutch torque of a SECA system. The proposed method is applicable to other manipulator systems that require asymptotic convergence of the state and the unknown inputs. This observer provides the estimated velocity as well as the reaction torque at the same time in which the actuator position signal is used only. Since the proposed observer can be used to monitor the reaction torque after the clutch makes contact, the PTOB plays the role of a balanced type torque sensor for actuator. This is the advantage of this approach compared with the driveline based-torque observer [3]–[6], [43] that is only available while the clutch is slipping.

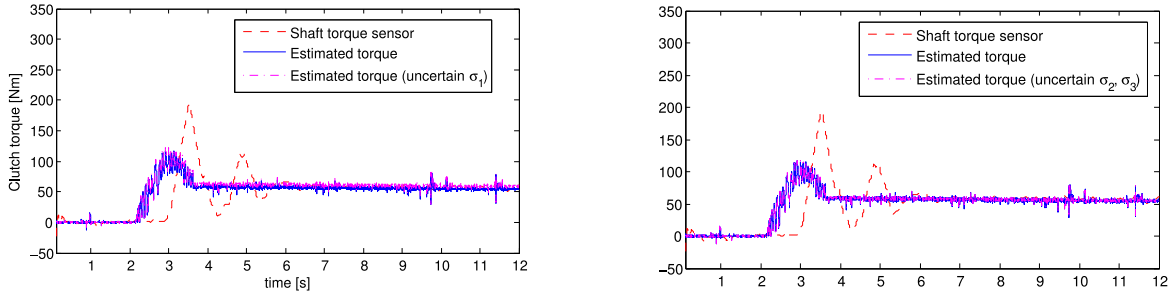

(a) (b)

Fig. 8. Clutch torque estimation by velocity signal-based observer with uncertain parameter: 8(a) σ_1, 8(b) σ_2 and σ_3 increased up to 20% from the nominal values.

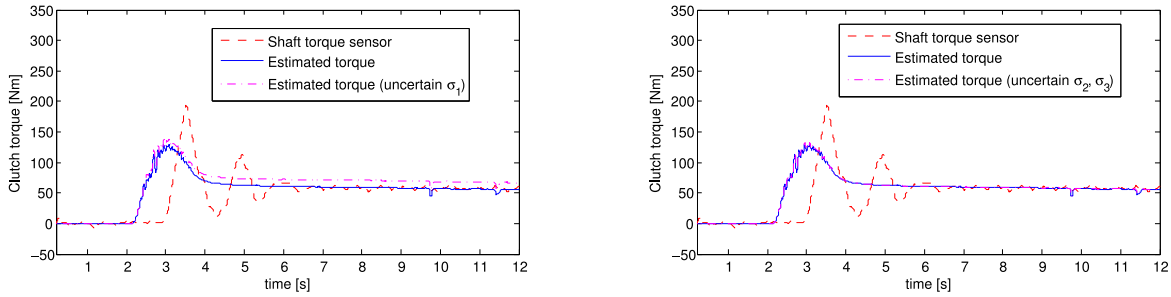

(a) (b)

Fig. 9. Clutch torque estimation by position signal-based observer with uncertain parameter: 9(a) σ_1, 9(b) σ_2 and σ_3 increased up to 20% from the nominal values.

In future works, a sensorless engagement control of a SECA will be developed by utilizing the proposed reaction torque observer. It may be helpful to reduce the impact force at the contact moment. The parameter design issues for selecting the observer gains need to be considered along the control gains.

APPENDIX
PROOF OF LEMMA 1

The integration of N_2 in (53) is given as

$$\int_0^t N_2(\tau)d\tau = \int_0^t r_2(\tau)\left(\dot{d}(\tau) - k_1 \mathrm{sgn}(\xi_2^*(\tau))\right)d\tau. \quad (81)$$

Using the definition (47), (81) can be rewritten by

$$\int_0^t N_2(\tau)d\tau = \int_0^t \frac{d\xi_2(\tau)}{d\tau}\dot{d}(\tau)d\tau - \int_0^t \dot{\xi}_2(\tau)k_1\mathrm{sgn}(\xi_2^*(\tau))d\tau + \int_0^t \xi_2\left(\dot{d}(\tau) - k_1\mathrm{sgn}(\xi_2^*(\tau))\right)d\tau. \quad (82)$$

The first term of (82) can be integrated by parts.

$$\int_0^t N_2(\tau)d\tau = \xi_2(t)\dot{d}(t) - \xi_2(0)\dot{d}(0) - \int_0^t \dot{\xi}_2(\tau)k_1\mathrm{sgn}(\xi_2^*(\tau))d\tau + \int_0^t \xi_2(\tau)R(\tau)d\tau \quad (83)$$

where $R(t) := \dot{d}(t) + \ddot{d}(t) - k_1\mathrm{sgn}(\xi_2^*(t))$ is used for notational simplicity. Adding and subtracting the terms

$$\int_0^t \dot{\xi}_2^*(\tau)k_1\mathrm{sgn}(\xi_2^*(\tau))d\tau + \xi_2^*\dot{d} + \int_0^t \xi_2(\tau)R(\tau)d\tau \quad (84)$$

to (83) and some algebraic manipulations yield the expression

$$\begin{aligned}\int_0^t N_2(\tau)d\tau = {} & (\xi_2(t) - \xi_2^*(t))\dot{d}(t) + \xi_2^*(t)\dot{d}(t) - \xi_2(0)\dot{d}(0) \\ & - \int_0^t \frac{d(\xi_2 - \xi_2^*)}{d\tau}k_1\mathrm{sgn}(\xi_2^*(\tau))d\tau \\ & - \int_0^t \frac{d\xi_2^*(\tau)}{d\tau}k_1\mathrm{sgn}(\xi_2^*(\tau))d\tau \\ & + \int_0^t (\xi_2 - \xi_2^*)R(\tau)d\tau + \int_0^t \xi_2^*(\tau)R(\tau)d\tau. \quad (85)\end{aligned}$$

In (42), the low-pass filter is employed to obtain ξ_2^* signal. When the ϵ is chosen to be small sufficiently, it follows that $\lim_{\epsilon\to 0}\xi_2^* = L\phi_1\xi_1$. It is clear that $\xi_2 - \xi_2^* = -L\xi_1$ and $\mathrm{sgn}(\xi_2^*) = \mathrm{sgn}(L\phi_1\xi_1)$

$$\begin{aligned}\int_0^t N_2(\tau)d\tau \le {} & -Le_1\dot{d}(t) - \xi_2(0)\dot{d}(0) \\ & + \int_0^t \frac{d(L\xi_1)}{d\tau}k_1\mathrm{sgn}(L\phi_1\xi_1)d\tau - \int_0^t \frac{d\xi_2^*}{d\tau}k_1\mathrm{sgn}(\xi_2^*)d\tau \\ & + \int_0^t (\xi_2^* - L\xi_1)R(\tau)d\tau. \quad (86)\end{aligned}$$

After integrating the third and fourth terms in (86), the expression (86) is rewritten as

$$\int_0^t N_2(\tau)d\tau \leq (\xi_2^* - L\xi_1)\left(\dot{d}(t) - k_1\right) + \int_0^t (\xi_2^* - L\xi_1)R(\tau)d\tau + \zeta_d \qquad (87)$$

where ζ_d is defined in (54). If k_1 satisfies the condition (59) and ϵ is sufficiently small, it can be concluded that (60) holds.

REFERENCES

[1] M. Pisaturo, M. Cirrincione, and A. Senatore, "Multiple constrained MPC design for automotive dry clutch engagement," *IEEE/ASME Trans. Mechatron.*, vol. 20, no. 1, pp. 469–480, Feb. 2015.

[2] A. Myklebust and L. Eriksson, "Modeling, observability, and estimation of thermal effects and aging on transmitted torque in a heavy duty truck with a dry clutch," *IEEE/ASME Trans. Mechatronics*, vol. 20, no. 1, pp. 61–72, Feb. 2015.

[3] R. A. Masmoudi and J. K. Hedrick, "Estimation of vehicle shaft torque using nonlinear observers," *Trans. ASME, J. Dyn. Syst. Meas. Contr.*, vol. 114, no. 3, pp. 394–400, 1992.

[4] K. Yi, B.-K. Shin, and K.-I. Lee, "Estimation of turbine torque of automatic transmissions using nonlinear observers," *Trans. ASME, J. Dyn. Syst. Meas. Contr.*, vol. 122, no. 2, pp. 276–283, 2000.

[5] P. Li, T. Jin, and X. Du, "Torque observer modelling for vehicle transmission shifting processing based on neural networks," in *Proc. 17th IFAC World Congr.*, Seoul, Korea, Jul. 2008, pp. 16039–16044.

[6] J. Kim and S. Choi, "Control of dry clutch engagement for vehicle launches via a shaft torque observer," in *Proc. Amer. Control Conf.*, Baltimore, MD, USA, Jun. 2010, pp. 676–681.

[7] H. Langjord, T. A. Johansen, S. R. Snare, and C. Bratli, "Estimation of electropneumatic clutch actuator load characteristics," presented at the 17th IFAC World Congr., Seoul, Korea, 2008.

[8] G. O. K. H. Langjord and T. A. Johansen, "Nonlinear observer and parameter estimation for electropneumatic clutch actuator," presented at the 8th IFAC Symp. Nonlinear Control Syst., Bologna, Italy, 2010.

[9] H. Langjor, G. O. Kaasa, and T. A. Johansen, "Adaptive observer-based switched controller for electropneumatic clutch actuator with position sensor," presented at the 18th IFAC World Congr., Milan, Italy, Sep. 2011.

[10] H. Langjord, T. Johansen, and J. Hespanha, "Switched control of an electropneumatic clutch actuator using on/off valves," in *Proc. Amer. Control Conf.*, Jun. 2008, pp. 1513–1518.

[11] H. Langjord and T. Johansen, "Dual-mode switched control of an electropneumatic clutch actuator," *IEEE/ASME Trans. Mechatronics*, vol. 15, no. 6, pp. 969–981, Dec. 2010.

[12] B. Gao, H. Chen, Q. Liu, and K. Sanada, "Clutch slip control of automatic transmissions: A nonlinear feedforward-feedback design," in *Proc. IEEE Int. Conf. Control Appl.*, 2010, pp. 884–889.

[13] B. Gao, H. Chen, H. Zhao, and K. Sanada, "A reduced-order nonlinear clutch pressure observer for automatic transmission," *IEEE Trans. Contr. Syst. Technol.*, vol. 18, no. 2, pp. 446–453, Mar. 2010.

[14] X. Song and Z. Sun, "Pressure-based clutch control for automotive transmissions using a sliding-mode controller," *IEEE/ASME Trans. Mechatronics*, vol. 17, no. 3, pp. 534–546, Jun. 2012.

[15] J. Kim and S. B. Choi, "Design and modeling of a clutch actuator system with self-energizing mechanism," *IEEE/ASME Trans. Mechatronics*, vol. 16, no. 5, pp. 953–966, Oct. 2011.

[16] K. Ohnishi, M. Shibata, and T. Murakami, "Motion control for advanced mechatronics," *IEEE/ASME Trans. Mechatronics*, vol. 1, no. 1, pp. 56–67, Mar. 1996.

[17] T. Murakami, F. Yu, and K. Ohnishi, "Torque sensorless control in multidegree-of-freedom manipulator," *IEEE Trans. Ind. Electron.*, vol. 40, no. 2, pp. 259–265, Apr. 1993.

[18] K. Ohishi, T. Miyazaki, K. Inomata, H. Yanagisawa, D. Koide, and H. Tokumaru, "Robust tracking servo system considering force disturbance for the optical disk recording system," *IEEE Trans. Ind. Electron.*, vol. 53, no. 3, pp. 838–847, Jun. 2006.

[19] S. Katsura, Y. Matsumoto, and K. Ohnishi, "Realization of 'Law of action and reaction' by multilateral control," *IEEE Trans. Ind. Electron.*, vol. 52, no. 5, pp. 1196–1205, Oct. 2005.

[20] S. Katsura, J. Suzuki, and K. Ohnishi, "Pushing operation by flexible manipulator taking environmental information into account," *IEEE Trans. Ind. Electron.*, vol. 53, no. 5, pp. 1688–1697, Oct. 2006.

[21] S. Katsura, K. Ohnishi, and K. Ohishi, "Transmission of force sensation by environment quarrier based on multilateral control," *IEEE Trans. Ind. Electron.*, vol. 54, no. 2, pp. 898–906, Apr. 2007.

[22] C. Mitsantisuk, S. Katsura, and K. Ohishi, "Kalman-filter-based sensor integration of variable power assist control based on human stiffness estimation," *IEEE Trans. Ind. Electron.*, vol. 56, no. 10, pp. 3897–3905, Jun. 2009.

[23] C. Mitsantisuk, K. Ohishi, and S. Katsura, "Estimation of action/reaction forces for the bilateral control using Kalman filter," *IEEE Trans. Ind. Electron.*, vol. 59, no. 11, pp. 4383–4393, Nov. 2012.

[24] X. Chen, C.-Y. Su, and T. Fukuda, "A nonlinear disturbance observer for multivariable systems and its application to magnetic bearing systems," *IEEE Trans. Contr. Syst. Technol.*, vol. 12, no. 4, pp. 569–577, Jul. 2004.

[25] W.-H. Chen, "Disturbance observer based control for nonlinear systems," *IEEE/ASME Trans. Mechatronics*, vol. 9, no. 4, pp. 706–710, Dec. 2004.

[26] K. C. Veluvolu and Y. C. Soh, "High-gain observers with sliding mode for state and unknown input estimations," *IEEE Trans. Ind. Electron.*, vol. 56, no. 9, pp. 3386–3393, Sep. 2009.

[27] B. Xian, D. Dawson, M. de Queiroz, and J. Chen, "A continuous asymptotic tracking control strategy for uncertain nonlinear systems," *IEEE Trans. Automat. Contr.*, vol. 49, no. 7, pp. 1206–1211, Jul. 2004.

[28] P. Patre, W. MacKunis, C. Makkar, and W. Dixon, "Asymptotic tracking for systems with structured and unstructured uncertainties," *IEEE Trans. Contr. Syst. Technol.*, vol. 16, no. 2, pp. 373–379, Mar. 2008.

[29] P. Patre, W. MacKunis, K. Dupree, and W. Dixon, "Modular adaptive control of uncertain euler-lagrange systems with additive disturbances," *IEEE Trans. Automat. Contr.*, vol. 56, no. 1, pp. 155–160, Jan. 2011.

[30] M. McIntyre, W. Dixon, D. Dawson, and I. Walker, "Fault identification for robot manipulators," *IEEE Trans. Robot. Automat.*, vol. 21, no. 5, pp. 1028–1034, Oct. 2005.

[31] C. Makkar, G. Hu, W. Sawyer, and W. Dixon, "Lyapunov-based tracking control in the presence of uncertain nonlinear parameterizable friction," *IEEE Trans. Automat. Contr.*, vol. 52, no. 10, pp. 1988–1994, Oct. 2007.

[32] J. Kim and S. B. Choi, "Self-energizing clutch actuator system: Basic concept and design," in *Proc. FISITA World Automotive Congr.*, no. FISITA2010-SC-P-23, May 2010.

[33] J. Kim and S. B. Choi, "Adaptive force control of autmotive clutch actuator system with self-energizing effect," presented at the 18th IFAC World Congr., Milano, Italy, Aug. 2011.

[34] A. Tarasow, G. Wachsmuth, J. Lemieux, R. Serway, and C. Bohn, "Online estimation of time-varying torque characteristics of automotive clutches using a control oriented model," in *Proc. Amer. Control Conf.*, 2013, pp. 6752–6757.

[35] A. Atassi and H. Khalil, "A separation principle for the stabilization of a class of nonlinear systems," *IEEE Trans. Automat. Contr.*, vol. 44, no. 9, pp. 1672–1687, Sep. 1999.

[36] A. Teel and L. Praly, "Global stabilizability and observability imply semi-global stabilizability by output feedback," *Syst. Control Lett.*, vol. 22, no. 5, pp. 313–325, 1994.

[37] S. Katsura, Y. Matsumoto, and K. Ohnishi, "Modeling of force sensing and validation of disturbance observer for force control," *IEEE Trans. Ind. Electron.*, vol. 54, no. 1, pp. 530–538, Feb. 2007.

[38] H. Shim and Y. Joo, "State space analysis of disturbance observer and a robust stability condition," in *Proc. IEEE Conf. Decision Control*, New Orleans, LA, USA, Dec. 2007, pp. 2193–2198.

[39] V. Utkin, "Application of equivalent control method to the systems with large feedback gain," *IEEE Trans. Automat. Contr.*, vol. AC-23, no. 3, pp. 484–486, Jun. 1978.

[40] V. Utkin, J. Guldner, and J. Shi, *Sliding Mode Control in Electromechanical Systems*. New York, NY, USA: Taylor & Francis, 1999.

[41] H. Khalil, *Nonlinear System*. 3rd ed. Upper Saddle River, NJ, USA: Prentice-Hall, 2002.

[42] J. J. Oh, S. B. Choi, and J. Kim, "Driveline modeling and estimation of individual clutch torque during gear shifts for dual clutch transmission," *Mechatronics*, vol. 24, no. 5, pp. 449–463, 2014.

[43] P. Dolcini, C. Canudas de Wit, and H. Béchart, "Lurch avoidance strategy and its implementation in AMT vehicles," *Mechatronics*, vol. 18, no. 5/6, pp. 289–300, Jun. 2008.

Jinsung Kim (S'10–M'13) received the Ph.D. degree in mechanical engineering from Korea Advanced Institute of Science and Technology (KAIST), Daejeon, Korea, 2013.

He is currently a Senior Research Engineer with Research and Development Center, Hyundai Motor Company, Seoul, Korea, where he designed clutch control algorithms of a seven-speed dual clutch transmissions for production vehicles. His current research interests include automotive systems, nonlinear control, and integrated design and control of complex mechanical systems.

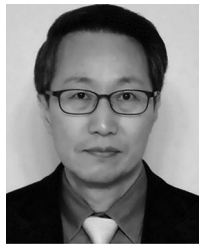

Seibum B. Choi (M'09) received the B.S. degree in mechanical engineering from Seoul National University, Seoul, Korea, the M.S. degree in mechanical engineering from Korea Advanced Institute of Science and Technology (KAIST), Daejeon, Korea, and the Ph.D. degree in controls from the University of California, Berkeley, CA, USA, in 1993.

From 1993 to 1997, he had worked on the development of automated vehicle control systems at the Institute of Transportation Studies at the University of California, Berkeley. Through 2006, he was with TRW, MI, where he worked on the development of advanced vehicle control systems. Since 2006, he has been with the faculty of the Mechanical Engineering Department at KAIST. His research interests include fuel saving technology, vehicle dynamics and control, and active safety systems.